Catalytic Oligomerization of Ethylene to Higher Linear α-Olefins Promoted by Cationic Group 4 Cyclopentadienyl-Arene Active Catalysts: A DFT Investigation Exploring the Influence of Electronic Factors on the Catalytic Properties by Modification of the Hemilabile Arene Functionality

Sven Tobisch*,† and Tom Ziegler‡

Institut für Anorganische Chemie der Martin-Luther-Universität Halle-Wittenberg, Fachbereich Chemie, Kurt-Mothes-Strasse 2, D-06120 Halle, Germany, and Department of Chemistry, University of Calgary, University Drive 2500, Calgary, Alberta, Canada T2N 1N4

Received March 15, 2004

Hessen and co-workers described Ti-based precatalysts of the title class bearing a hemilabile ancillary arene functionality for ethylene trimerization. The analogues with the heavier group 4 metals Zr and Hf as the active center have been recently explored computationally. This study suggested the Zr-based system as a promising catalyst for production of an oligomer mixture containing 1-octene besides the prevalent 1-hexene. Herein, we have presented a detailed computational analysis of the influence of modifications of the hemilabile arene functionality on the catalytic abilities of cationic group 4 [(η^5-Cp-(CMe_2R'-bridge)-$C_6H_yR_x$)$M^{II}(C_2H_4)_2$]$^+$ active species (M = Zr, Hf) for linear ethylene oligomerization, employing a gradient-corrected DFT method. This comprised the arene substitution with prototypical electron-releasing (R = Me) and electron-withdrawing (R = F, CF_3) groups in various combinations and also the enlargement of the Cp-arene connecting bridge by an additional methylene group (R′ = CH_2). The overall barrier connected with metallacycle growth has been analyzed as being decisively determined by the strength of the M^{IV}−arene interaction in the metallacycle precursor, with the first arene displacement by incoming ethylene as the major contribution to the relative kinetics. For catalysts bearing an extended C_2-bridge or a donor-substituted arene functionality this interaction becomes increased, thereby acting to reduce the tendency for ethylene π-adduct formation and also increasing the insertion barrier. The opposite influence has been found for substituents that are electron-withdrawing. The barrier for metallacycle decomposition is essentially controlled by the ability of the arene group to stabilize the transition state coordinatively. The donor and acceptor abilities of the substituent have been described as the crucial electronic factor that acts to accelerate and retard, respectively, this process. Among the two crucial elementary processes, the ethylene insertion has been found as being distinctly affected to a larger extent by the probed modifications of the hemilabile arene functionality. The influence of these modifications, in modulating the oligomer product composition and the catalytic activity, has been elucidated.

Introduction

Higher (C_4−C_{20}) linear α-olefins have become increasingly important for polymer manufacturing[1,2] as monomers (C_{10} for production of poly-α-olefins) and as comonomers (C_4−C_8 for generation of linear low-density LLDPE[3] polyethylene) and also as additives for high-density HDPE polyethylene production. Apart from their application as polyolefin building blocks, higher linear α-olefins are used for production of surfactants (C_{10}−C_{18})[1c,e] and for plasticizer (C_6−C_{10}) manufacturing.[1c,e]

* To whom correspondence should be addressed. E-mail: tobisch@chemie.uni-halle.de.
† Martin-Luther-Universität Halle-Wittenberg.
‡ University of Calgary.

(1) (a) Weissermal, K.; Arpe, H.-J. In *Industrial Organic Chemistry. Important Raw Materials and Intermediates*; Verlag Chemie: Weinheim, 1978. (b) Parshall, G. W.; Ittel, S. D. In *Homogeneous Catalysis, The Applications and Chemistry of Catalysis by Soluble Transition Metal Complexes*; John Wiley & Sons: New York, 1992; p 56. (c) Al-Jarallah, A. H.; Anabtawi, J. A.; Siddiqui, M. A. B.; Aitani, A. M.; Al-Sadoun, A. W. *Catal. Today* **1992**, *14*, 1. (d) Bhaduri, S.; Mukesh, D. In *Homogeneous Catalysis, Mechanisms and Industrial Applications*; John Wiley & Sons: New York, 2000; pp 142−147. (e) Vogt, D. Oligomerization of Ethylene to Higher Linear α-Olefins. In *Applied Homogeneous Catalysis with Organometallic Complexes*; Cornils, B., Herrmann, W. A., Eds.; VCH: Weinheim, Germany, 2002; pp 240−253.

(2) (a) Tait, P. J. T.; Berry, I. G. In *Comprehensive Polymer Science*; Eastmond, G. C., Ledwith, A., Russo, S., Sigwalt, P., Eds.; Pergamon: Oxford, U.K., 1989; Vol. 4, p 575. (b) *Encyclopedia of Polymer Science and Engineering*; Mark, H. F., Bikales, N. B., Overberger, C. G., Menges, G., Kroschwitz, J. I., Eds.; John Wiley & Sons: New York, 1986; Vol. 6, p 429.

(3) Hennico, A.; Leonard, J.; Forestire, A.; Glaize, Y. *Hydrocarbon Process* **1990**, *69*, 73.

10.1021/om0498100 CCC: $27.50
Publication on Web 07/21/2004

Among the many processes known for production of α-olefins, nowadays oligomerization of the less expensive ethylene is the predominant route,[1c,e,4] with the Shell higher olefin process (SHOP)[5] as the predominant industrial process.

The oligomerization of ethylene, which is promoted by a variety of catalysts,[6,7] typically gives a broad Schulz−Flory distribution[8] of α-olefins having different chain lengths, which have to be separated via fractional distillation. Recently, intensive research in both academia and industry has targeted the development of catalyst systems for selective ethylene oligomerization for specific desirable α-olefins. There have been several recent reports of the selective ethylene trimerization to 1-hexene with catalysts that are based on chromium,[9] tantalum,[10] and titanium.[11,12]

In a recent work, Hessen and co-workers described mono(cyclopentadienylarene)titanium systems bearing a hemilabile ancillary arene ligand as generators for a class of active catalysts for ethylene trimerization.[12a,b] Within this class, the cationic $[(\eta^5$-Cp-$(CMe_2$-bridge)-$C_6H_5)Ti^{IV}$-$(alkyl)_2]^+$ species with a dimethyl-substituted C_1-bridge connecting the Cp ring with the pendant arene functionality has been observed as one of the most active precatalysts that affords 1-hexene with high selectivity.[12b] We have recently reported comprehensive theoretical mechanistic studies on the ethylene oligomerization with this Ti precatalyst as well as for the related Zr and Hf systems.[13] This allowed us to support a mechanism involving metallacycle intermediates, first proposed[14,15] and recently conclusively corroborated[9j] for Cr catalysts as being favorable over a Cossee/Arlman-type mechanism,[16] and to provide a detailed insight into the important factors that are responsible for the observed high selectivity of the Ti catalyst for ethylene trimerization.

A tentative catalytic cycle for the Ti-mediated ethylene oligomerization, involving metallacycle intermediates of various ring sizes, suggested by Hessen and co-workers[12a,b] in great similarity to the original mechanistic proposal of Briggs and Jolly for Cr-based catalysts,[14,15] has been verified recently in essential aspects by computational studies.[13a,17] The suggested refined catalytic cycle for oligomerization supported by the Zr and Hf analogues[13b] is displayed in Scheme 1. The bis(ethylene)−M^{II} complex represents the active catalyst species that is generated via a smooth initial process of precatalyst activation. The first step consists of the oxidative coupling of two ethylenes, giving rise to the metalla(IV)cyclopentane. Repeated ethylene uptake and consecutive insertion into the M^{IV}−C bond of the metallacycle increases their ring size. The various α-olefins are generated through decomposition of the respective metallacycle intermediate, following two distinct mechanisms. The conformationally flexible cycles starting with the metalla(IV)cycloheptane preferably decompose through the concerted transition-metal-assisted β-H transfer, while a stepwise mechanism comprised of β-H abstraction and subsequent reductive CH elimination with an intervening alkenyl-hydride−M^{IV} species is operative for the conformationally rigid metalla(IV)-cyclopentane. Due to the unfavorable kinetics connected with the stepwise decomposition, for the five-membered cycle the further growth by ethylene insertion is the more likely process, thereby precluding formation of 1-butene (cf. Scheme 1). For the next two larger seven- and nine-membered metallacycles, however, the competing growth and decomposition steps have similar barriers, which indicates that the two processes should occur with comparable probabilities. The concerted β-H transfer becomes significantly retarded kinetically relative to the insertion step for metallacycles bigger than the nine-membered ring, which are therefore indicated as having a distinctly higher ability for further growth, while the decomposition into the corresponding α-olefins is almost entirely suppressed. Accordingly, the Zr- and Hf-based systems are indicated to not promote the

(4) (a) Onsager, O.-T.; Johansen, J. E. In *The Chemistry of the Metal-Carbon Bond*; Hartley, F. R., Patai, F. R., Eds.; John Wiley & Sons: Chicester, U.K., 1986; Vol. 3 p 205. (b) Skupinska, J. *Chem. Rev.* **1991**, *91*, 613. (c) Olivier-Bourbigou, H.; Saussine, L. Dimerization and Codimerization. In *Applied Homogeneous Catalysis with Organometallic Complexes*; Cornils, B., Herrmann, W. A., Eds.; VCH: Weinheim, Germany, 2002; pp 253−265.

(5) (a) Keim, W.; Kowaldt, F. H. *Erdöl Erdgas Kohle* **1978**, *78*−*79*, 453. (b) Keim, W.; Kowaldt, F. H.; Goddard, R.; Krüger, C. *Angew. Chem., Int. Ed. Engl.* **1978**, *17*, 466. (c) Freitas, E. R.; Gum, C. R. *Chem. Eng. Prog.* **1979**, *75*, 73. (d) Keim, W. *Chem. Ing. Technol.* **1984**, *56*, 850. (e) Keim, W. *New J. Chem.* **1987**, *11*, 531. (f) Keim, W. *Angew. Chem., Int. Ed. Engl.* **1990**, *29*, 235. (g) Keim, W. *Makromol. Chem. Macromol. Symp.* **1993**, *66*, 225. (h) Vogt, D. SHOP Process. In *Aqueous-Phase Organometallic Catalysts, Concepts and Applications*; Cornils, B., Herrmann, W. A., Eds.; VCH: Weinheim, Germany, 1998; pp 541−547.

(6) For past reviews see: (a) Keim, W.; Behr, A.; Röper, M. Alkene and Alkyne Oligomerization, Cooligomerization and Telomerization Reactions. In *Comprehensive Organometallic Chemistry*; Wilkinson, G., Stone, F. G. A., Abel, E. W., Eds.; Pergamon: New York, 1982; Vol. 8, pp 371−462. (b) Jolly, P. W. Nickel-Catalyzed Oligomerization of Alkenes and Related Reactions. In *Comprehensive Organometallic Chemistry*; Wilkinson, G., Stone, F. G. A., Abel, E. W., Eds.; Pergamon: New York, 1982; Vol. 8, pp 615−647.

(7) For recent reviews see: (a) Britovsek, G. J. P.; Gibson, V. C.; Wass, D. F. *Angew. Chem., Int. Ed.* **1999**, *38*, 428. (b) Ittel, S. D.; Johnson, L. K.; Brookhart, M. *Chem. Rev.* **2000**, *100*, 1169. (c) Mecking, S. *Coord. Chem. Rev.* **2000**, *203*, 325. (d) Mecking, S. *Angew. Chem., Int. Ed.* **2001**, *40*, 534. (e) Gibson, V. C.; Spitzmesser, S. K. *Chem. Rev.* **2003**, *103*, 283.

(8) (a) Flory, P. J. *J. Am. Chem. Soc.* **1940**, *62*, 1561. (b) Schulz, G. V. *Z. Phys. Chem., Abt. B* **1935**, *30*, 379. (c) Schulz, G. V. *Z. Phys. Chem., Abt. B* **1939**, *43*, 25.

(9) (a) Hogan, J. P. *J. Polym. Sci. A* **1970**, *8*, 2637. (b) Manyik, R. M.; Walker, W. E.; Wilson, T. P. *J. Catal.* **1977**, *47*, 197. (c) Yang, Y.; Kim, H.; Lee, J.; Paik, H.; Jang, H. G. *Appl. Catal. A Gen.* **2000**, *193*, 29. (d) Köhn, R. D.; Haufe, M.; Kociok-Köhn, G.; Grimm, S.; Wasserscheid, P.; Keim, W. *Angew. Chem., Int. Ed.* **2000**, *39*, 4337. (e) Monoi, T.; Sasaki, Y. *J. Mol. Catal. A: Chem.* **2002**, *187*, 135. (f) Carter, A.; Cohen, S. A.; Cooley, N. A.; Murphy, A.; Scutt, J.; Wass, D. F. *Chem. Commun.* **2002**, 858. (g) McGuinness, D. S.; Wasserscheid, P.; Keim, W.; Morgan, D.; Dixon, J. T.; Bollmann, A.; Maumela, H.; Hess, F.; Englert, U. *J. Am. Chem. Soc.* **2003**, *125*, 5272. (h) McGuinness, D. S.; Wasserscheid, P.; Keim, W.; Hu, Ch.; Englert, U.; Dixon, J. T.; Grove, C. *Chem. Commun.* **2003**, 334. (i) Morgan, D. H.; Schwikkard, S. L.; Dixon, J. T.; Nair, J. J.; Hunter, R. *Adv. Synth. Catal.* **2003**, *345*, 939. (j) Agapi, T.; Schofer, S. J.; Labinger, J. A.; Bercaw, J. E. *J. Am. Chem. Soc.* **2004**, *126*, 1304.

(10) Andes, C.; Harkins, S. B.; Murtuza, K. O.; Sen. A. *J. Am. Chem. Soc.* **2001**, *123*, 7423.

(11) Pellecchia, C.; Pappalardo, D.; Oliva, L.; Mazzeo, M.; Gruter, G.-J. *Macromolecules* **2000**, *33*, 2807.

(12) (a) Deckers, P. J. W.; Hessen, B.; Teuben, J. H. *Angew. Chem., Int. Ed.* **2001**, *40*, 2516. (b) Deckers, P. J. W.; Hessen, B.; Teuben, J. H. *Organometallics* **2002**, *21*, 5122. (c) The actual reaction conditions for the Ti-catalyzed selective trimerization of ethylene to 1-hexene: 30 °C, ethylene pressure 5 bar, toluene as solvent.

(13) (a) Tobisch, S.; Ziegler, T. *Organometallics* **2003**, *22*, 5392. (b) Tobisch, S.; Ziegler, T. *J. Am. Chem. Soc.* **2004**, *126*, accepted.

(14) Briggs, J. R. *Chem. Soc., Chem. Commun.* **1989**, 674.

(15) (a) Jolly, P. W. *Acc. Chem. Res.* **1996**, *29*, 544. (b) Emrich, R.; Heinemann, O.; Jolly, P. W.; Krüger, C.; Verhovnik, G. P. J. *Organometallics* **1997**, *16*, 1511.

(16) (a) Cossee, P. *J. Catal.* **1964**, *3*, 80. (b) Arlman, E. J.; Cossee, P. *J. Catal.* **1964**, *3*, 99.

(17) (a) Blok, A. N. J.; Budzelaar, P. H. M.; Gal, A. W. *Organometallics* **2003**, *22*, 2564. (b) de Bruin, T. J. M.; Magna, L.; Raybaud, P.; Toulhoat, H. *Organometallics* **2003**, *22*, 3404.

Scheme 1. Theoretically Refined Catalytic Cycle for the Linear Oligomerization of Ethylene Mediated by the Cationic Heavier Group 4 [(η^5-Cp-(bridge)-Ar)M^{II}(ethylene)$_2$]$^+$ Active Catalysts (M = Zr, Hf; Ar = Ph)[a,13b]

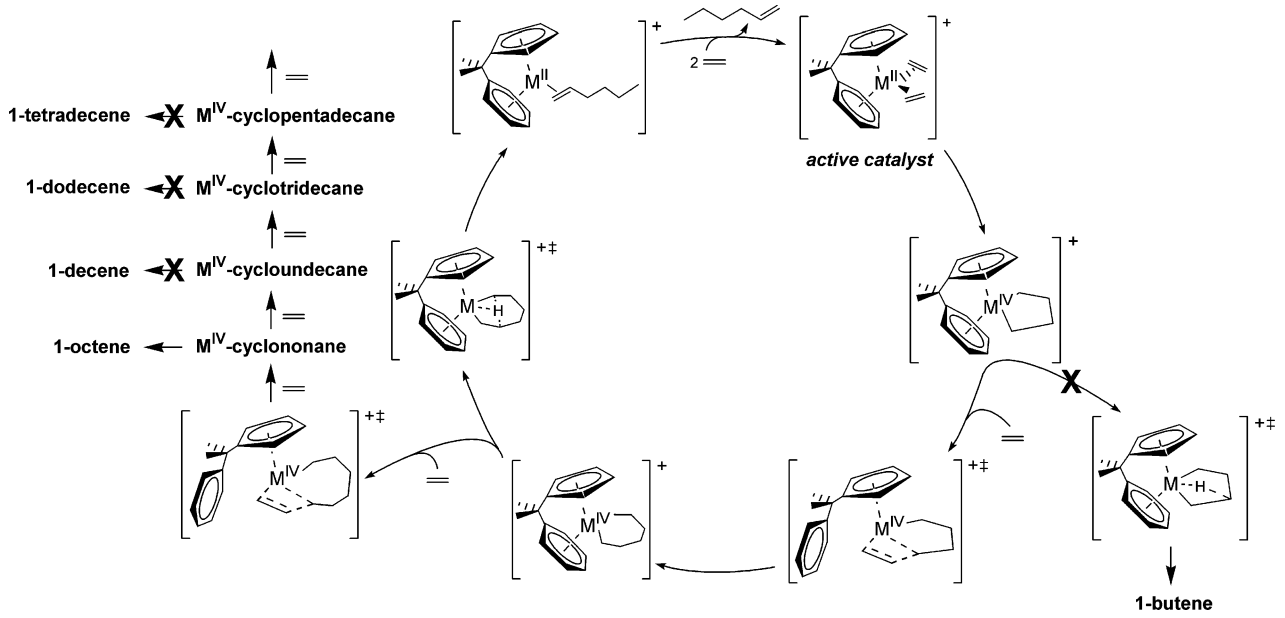

[a] Based on a proposal by Hessen et al. for the Ti-catalyzed process.[12a,b]

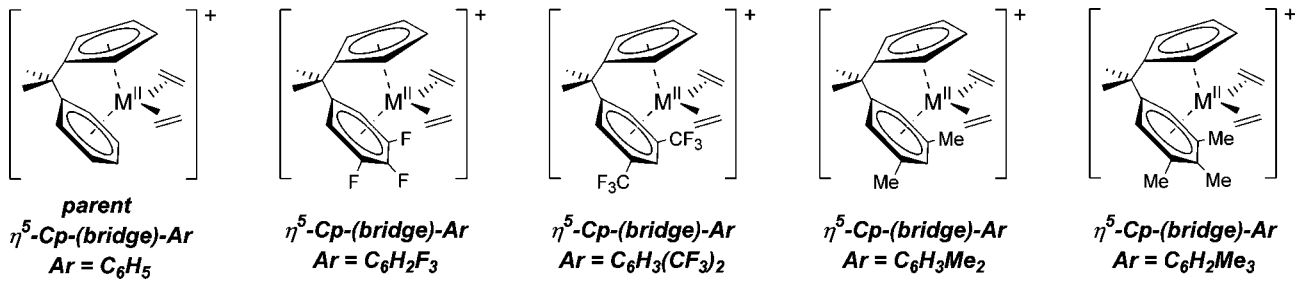

Figure 1. Explored substitution pattern of the hemilabile arene functionality of the [(η^5-C_5H_4-(CMe_2R'-bridge)-$C_6H_xR_y$)-M^{II}(ethylene)$_2$]$^+$ (M = Zr, Hf) active catalyst complex, exemplified for CMe_2-bridged systems.

ethylene oligomerization to a specific α-olefin, as the parent Ti trimerization catalyst does. The product mixture of the Zr-mediated process consists of 1-hexene as the prevalent oligomer together with 1-octene. 1-Butene and α-olefins of chain lengths C_{10}−C_{18}, however, should occur in only negligible portions. A similar composition of α-olefins having C_6−C_{18} chain lengths (albeit as a minor fraction) is generated by the Hf catalyts, but in contrast to the Zr system, here long chain oligomers/polymers are likely to be the prevalent fraction.[13b]

The present investigation continues our systematic theoretical exploration of the catalytic potential of group 4 mono(cyclopentadienylarene) compounds as catalysts for the oligomerization of ethylene. Herein, we report the detailed evaluation of the influence of electronic factors on the catalytic abilities of the heavier group 4 [(η^5-C_5H_4-(CMe_2R'-bridge)-$C_6H_xR_y$)M^{II}(ethylene)$_2$]$^+$ (M = Zr, Hf) active catalyst complexes for ethylene oligomerization. This comprises the substitution of the phenyl ring with prototypical electron-releasing (R = Me) and electron-withdrawing (R = F, CF_3) groups in various patterns and the enlargement of the C_1-bridge by an additional methylene group (R′ = CH_2). Catalysts bearing the pendant phenyl group of substitution pattern shown in Figure 1 were explored for both CMe_2- and CMe_2CH_2-bridged systems. The effect of the solvent and the counterion was neglected in the present study; the rationale behind them can be found elsewhere.[13a,b]

For the parent Ti-based systems, introduction of a larger CMe_2CH_2 C_2-bridge and a dimethyl-substituted phenyl ring still results in selective trimerization catalysts, but causes a remarkable decrease in the catalytic activity when compared to the above-mentioned most efficient Ti system.[12b] The related Zr and Hf catalysts are, however, hypothetical, as experimental studies on their catalytic properties have not been reported so far.

The present investigation will contribute to a deeper understanding of the catalytic structure−reactivity relationships for ethylene oligomerization promoted by the title class of group 4 catalysts. On the basis of these enhanced insights, it is our goal to suggest directions for promising modifications of Zr- and Hf-based catalysts aimed at modulating the oligomer product distribution to either the almost exclusive formation of 1-hexene or to maximize the 1-octene portion. The influence of temperature on the relative portions of the various oligomers has already been analyzed in our previous study.[13b]

Computational Details

All reported DFT calculations were performed by using the TURBOMOLE program package developed by Häser and

Ahlrichs.[18] The local exchange−correlation potential by Slater[19a,b] and Vosko et al.[19c] was augmented with gradient-corrected functionals for electron exchange according to Becke[19d] and correlation according to Perdew[19e] in a self-consistent fashion. This gradient-corrected density functional is usually termed BP86 in the literature. In recent benchmark computational studies it was shown that the BP86 functional gives results in excellent agreement with the best wave function-based methods available today, for the class of reactions investigated here.[20] The suitability of the DFT(BP86) method for the reliable description of the kinetic balance between the metallacycle growth and decomposition steps of the group 4 metal-assisted ethylene oligomerization has been previously demonstrated.[13b]

Basis sets of valence triple-ζ quality for all elements[21b] together with a quasirelativistic ECP for group 4 elements[22] were employed in the geometry optimization and transition state localization. The frequency calculations were conducted by using the same basis set for group 4 elements,[22] but split-valence basis sets[21a] for the main group elements for structures localized at this level. Further details of the computational procedure were reported elsewhere.[13b] The stationary points were identified exactly by the curvature of the potential energy surface at these points corresponding to the eigenvalues of the Hessian. All reported transition states possess exactly one negative Hessian eigenvalue, while all other stationary points exhibit exclusively positive eigenvalues. For the oligomerization to occur in liquid phase,[12c] the solvation entropy for olefin association and dissociation was approximated as being 2/3 of its gas-phase value. This is considered as a reliable estimate of the entropy contribution in condensed phase; further details were reported elsewhere.[13b]

To keep the notation consistent with previous studies,[13a,b] the key species of the oligomerization process were labeled with the following specific notation: viz., the metalla(IV)-cycloalkanes **XC**; the respective ethylene π-adducts **XC-E**; the α-olefin−M^{II} complex **XC-O**. The notation **X** = **7**, **9** was used to indicate whether seven- or nine-membered metallacycle intermediates, i.e., metalla(IV)cycloheptane or -nonane, respectively, were involved.

Results and Discussion

We shall focus here entirely on the examination of the competing growth and decomposition steps for metalla(IV)cycloheptane, **7C**, and -nonane, **9C**, intermediates. The kinetic balance between these elementary processes has been analyzed to determine the product distribution of oligomers in the valuable range of C_6−C_{18} chain lengths (vide supra).[13b] First, the influence of the variation of the catalyst backbone on the energy profile for the individual elementary steps will be evaluated, which should then allow us to suggest promising catalyst modifications aimed at improving their catalytic abilities.

I. Examination of Critical Elementary Processes. A. Growth of Metallacycle Intermediates. The key species for ethylene insertion into the M^{IV}−C bond of the metalla(IV)cycloheptane **7C** to afford the metalla(IV)cyclononane intermediate **9C** are displayed in Figure 2, exemplified for CMe_2- and CMe_2CH_2-bridged Zr catalysts with the parent arene functionality (Ar = C_6H_5). Table 1 collects the energetics for the growth of seven- and nine-membered zircona(IV)- and hafnia(IV)cycles, **7C** and **9C**, for all investigated catalysts. As revealed from the key species, the first ethylene uptake affording the encounter complexes **7C-E** and **9C-E**, respectively, comes at the expense of the M^{IV}−arene interaction. The ancillary phenyl group preferably adopts the η^1-mode for CMe_2-bridged metalla(IV)cycloalkanes, while it is only slightly unsymmetrical, thus more strongly coordinated for the systems with the larger CMe_2CH_2-bridge. As a general trend, for both C_1- and C_2-bridged species, the nearest M^{IV}−arene contact (i.e., M−C^{13} distance, cf. Figure 2) is found to become shorter/longer when the phenyl group is substituted with donor/acceptor ligands, respectively, relative to the parent systems (Ar = C_6H_5). This indicates that, in the absence of unfavorable steric interactions, electron-releasing substituents enhance the strength of the M^{IV}−arene interaction in **7C** and **9C**, while electron-withdrawing groups act to destabilize (vide infra). For the incoming ethylene to become accommodated, the hemilabile arene functionality has to be displaced from the immediate proximity of the metal in **7C-E** and **9C-E**, both of which are characterized as weak ethylene π-adducts (cf. Figure 2). The phenyl group still resides outside of the direct coordination sphere of the metal during the insertion process until it approaches the transition state, before becoming reattached after the TS decays into the next larger metalla(IV)cycloalkane. The overall highest barrier of the cycle growth process, comprised of the ethylene uptake and insertion steps, is connected with the insertion, while the uptake requires a significantly lower barrier.[13a]

As a general characteristic, the metallacycle growth process is accompanied by the displacement of the ancillary arene functionality by the incoming ethylene. Accordingly, the ethylene insertion should be kinetically more facile the weaker the M^{IV}−arene interaction in **7C** and **9C** is. On the other hand, a strongly coordinating phenyl group, which makes it more difficult for incoming ethylene to coordinate, should retard the insertion, or even preclude metallacycle growth entirely. This rationale is supported by the predicted stabilities of the ethylene encounter complexes **7C-E** and **9C-E** and also by the insertion barriers for the investigated catalysts (cf. Table 1). As for the parent systems, the extended C_2-bridge acts to adapt better to the larger ionic radius of Zr and Hf, resulting in a stronger coordination of the unsubstituted phenyl group in the metalla(IV)cycloalkanes (cf. Figure 2). This gives rise, independent of the metal and the cycle size, to a thermodynamically less favorable formation of the ethylene π-adducts **XC-E** and furthermore to higher insertion barriers for the CMe_2-CH_2-bridged systems when compared to the counterparts with a CMe_2-bridge. As a further general aspect,

(18) (a) Ahlrichs, R.; Bär, M.; Häser, M.; Horn, H.; Kölmel, C. *Chem. Phys. Lett.* **1989**, *162*, 165. (b) Treutler, O.; Ahlrichs, R. *J. Chem. Phys.* **1995**, *102*, 346. (c) Eichkorn, K.; Treutler, O.; Öhm, H.; Häser, M.; Ahlrichs, R. *Chem. Phys. Lett.* **1995**, *242*, 652.

(19) (a) Dirac, P. A. M. *Proc. Cambridge Philos. Soc.* **1930**, *26*, 376. (b) Slater, J. C. *Phys. Rev.* **1951**, *81*, 385. (c) Vosko, S. H.; Wilk, L.; Nussiar, M. *Can. J. Phys.* **1980**, *58*, 1200. (d) Becke, A. D. *Phys. Rev.* **1988**, *A38*, 3098. (e) Perdew, J. P. *Phys. Rev.* **1986**, *B33*, 8822.; *Phys. Rev. B* **1986**, *34*, 7406.

(20) Jensen, V. R.; Børve, K. *J. Comput. Chem.* **1998**, *19*, 947.

(21) (a) Schäfer, A.; Huber, C.; Ahlrichs, R. *J. Chem. Phys.* **1992**, *97*, 2571. (b) Schäfer, A.; Huber, C.; Ahlrichs, R. *J. Chem. Phys.* **1994**, *100*, 5829. (c) Eichkorn, K.; Treutler, O.; Öhm, H.; Häser, M.; Ahlrichs, R. *Chem. Phys. Lett.* **1995**, *240*, 283. (d) Eichkorn, K.; Weigend, F.; Treutler, O.; Ahlrichs, R. *Theor. Chim. Acta* **1997**, *97*, 119. (e) TURBOMOLE basis set library.

(22) (a) Dolg, M.; Wedig, U.; Stoll, H.; Preuss, H. *J. Chem. Phys.* **1987**, *86*, 866. (b) Andrae, D.; Häussermann, M.; Dolg, M.; Stoll, H.; Preuss, H. *Theor. Chim. Acta* **1990**, *77*, 123.

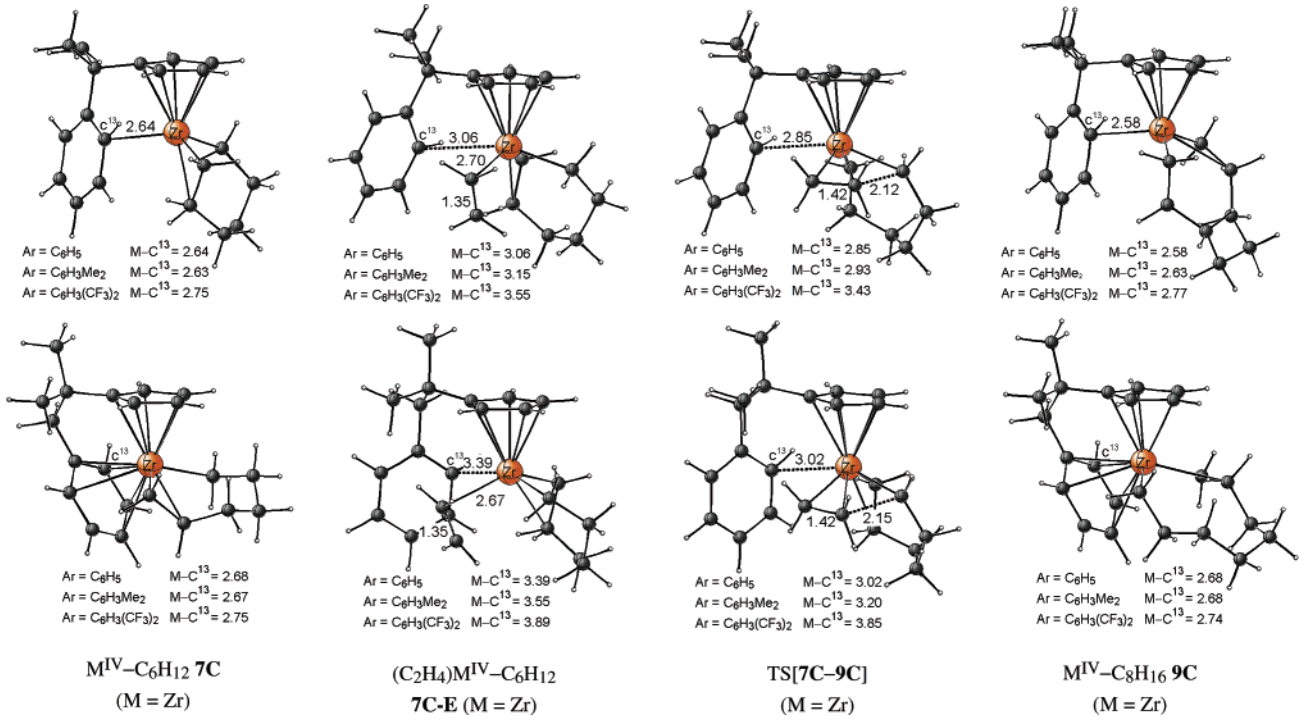

M^{IV}–C_6H_{12} **7C** (M = Zr) | $(C_2H_4)M^{IV}$–C_6H_{12} **7C-E** (M = Zr) | TS[**7C**–**9C**] (M = Zr) | M^{IV}–C_8H_{16} **9C** (M = Zr)

Figure 2. Selected geometric parameters (Å) of the optimized structures of key species for ethylene insertion into the M^{IV}–C bond of the metalla(IV)cycloheptane **7C** giving rise to the metalla(IV)-cyclononane intermediate **9C**, for CMe_2-bridged (top) and CMe_2CH_2-bridged (bottom) systems,[23] exemplified for the Zr catalyst with the parent (Ar = C_6H_5) arene functionality. The cutoff for drawing M–C bonds was arbitrarily set at 2.8 Å.

Table 1. Calculated Gibbs Free-Energy Profile (ΔG, $\Delta G^{\ddagger}$ in kcal mol^{-1}) for Growth of Group 4 Metallacycle Intermediates during the Linear Oligomerization of Ethylene Mediated by the Cationic $[(\eta^5\text{-}C_5H_4\text{-}(CMe_2R'\text{-bridge})\text{-}C_6H_xR_y)M^{II}(C_2H_4)_2]^+$ (M = Zr, Hf) Active Catalyst Complex[a,23]

cycle growth	arene functionality	$\Delta G_{\mathbf{XC-E}}$[b] M = Zr/Hf	$\Delta G^{\ddagger}$ M = Zr/Hf	ΔG M = Zr/Hf
M^{IV}–C_6 → M^{IV}–C_8H_{16}	C_6H_5	7.1/7.0	14.5/15.7	−5.3/−5.2
7C + C_2H_4 → **7C-E** → **9C**	$C_6H_2F_3$	4.9/4.7	12.7/13.9	−5.1/−4.9
CMe_2-bridge	$C_6H_3(CF_3)_2$	2.2/1.8	11.2/12.0	−4.0/−4.0
	$C_6H_3Me_2$	9.7/9.4	17.8/19.0	−6.4/−4.9
	$C_6H_2Me_3$	10.3/10.2	18.4/19.7	−6.5/−5.0
CMe_2CH_2-bridge	C_6H_5	11.7/10.9	18.3/19.8	−8.1/−6.2
	$C_6H_2F_3$	6.3/5.8	13.0/13.8	−8.0/−6.5
	$C_6H_3(CF_3)_2$	2.3/2.1	10.0/11.1	−7.5/−5.6
	$C_6H_3Me_2$	15.8/16.6	23.3/25.4	−7.3/−5.2
	$C_6H_2Me_3$	17.1/17.8	24.8/27.0	−6.6/−5.1
M^{IV}–C_8 → M^{IV}–$C_{10}H_{20}$	C_6H_5	12.6/12.4	17.3/17.4	−11.0/−10.4
9C + C_2H_4 → **9C-E** → **11C**	$C_6H_2F_3$	9.4/8.7	14.7/14.9	−11.0/−10.7
CMe_2-bridge	$C_6H_3(CF_3)_2$	4.7/3.2	10.5/10.7	−12.0/−11.3
	$C_6H_3Me_2$	15.7/14.0	20.6/19.2	−9.5/−10.4
	$C_6H_2Me_3$	16.2/14.5	21.1/19.8	−10.0/−10.5
CMe_2CH_2-bridge	C_6H_5	17.5/16.4	23.1/21.2	−9.8/−10.7
	$C_6H_2F_3$	13.1/11.5	17.5/16.1	−9.7/−10.4
	$C_6H_3(CF_3)_2$	6.5/5.5	12.5/11.3	−10.2/−10.8
	$C_6H_3Me_2$	20.4/21.0	26.8/25.7	−9.9/−10.8
	$C_6H_2Me_3$	22.0/21.0	27.3/26.7	−10.2/−10.6

[a] The activation and reaction free energies for individual processes are given for Zr-/Hf-based catalysts, respectively, relative to {corresponding metallacycle precursor **XC** + C_2H_4}. [b] Stabilization of the ethylene π-adduct **XC-E** (with X = 7, 9, respectively).

electron-donating substituents stabilize the M^{IV}–arene interaction in the metalla(IV)cycloalkane precursors (vide infra). They are therefore acting to reduce the ability to generate the encounter complex **XC-E** (i.e., their thermodynamically determined abundance) and will also make the insertion more difficult kinetically. The opposite behavior is predicted for substituents that are electron-withdrawing (cf. Table 1).

To get a more detailed insight into the substituent's influence, the overall insertion process has been divided into the monomer uptake and insertion steps and is analyzed by making use of a simple isodesmic relation, expressed in eq 1 for metalla(IV)cycloalkanes **XC**, as an example.[24]

$$\mathbf{XC}(\mathrm{Ar} = C_6H_5) + \text{toluene-R} \rightarrow \mathbf{XC}(\mathrm{Ar} = C_6H_xR_y) + \text{toluene} \quad (1)$$

Therein, R designates the substitution (R = Me, F, CF_3,

(23) M^{IV}–C_6H_{12} and M^{IV}–C_8H_{16} denotes the metalla(IV)cycloheptane **7C** and -nonane **9C** intermediates, respectively.

(24) A compilation of all data related to this analysis can be found in Tables S1 and S2, included in the Supporting Information, for the metallacycle growth and decomposition processes, respectively.

in different pattern, cf. Figure 1) of the parent arene functionality (Ar = C_6H_5) and of toluene, respectively. As clearly revealed from Table S2 (cf. Supporting Information package), electron-withdrawing/-donating substituents cause, in the absence of unfavorable steric interactions, a lower/higher stability of the metalla(IV)-cycloalkanes. This is seen to correlate well with the substituent's acceptor strength and the number of donor substituents.[25] The electronic stabilization of the group 4 metal−arene interaction by donor groups is well-known and is manifested by the several reported X-ray structures, with the strongly basic C_6Me_5-substituted arene group as a prime example of low-valent and high-valent complexes.[26] The relative thermodynamic abundance of the encounter complexes **XC-E** with a donor/acceptor-functionalized phenyl group is also predicted to follow a regular trend. Furthermore, the first phenyl group displacement during the ethylene uptake is seen to contribute to a major extent in the variation of the overall rate of ring extension. On the other hand, the intrinsic insertion barrier (i.e., $\Delta G_{int}^{\ddagger}$, relative to the corresponding ethylene π-adduct **XC-E**) is less affected by electronic factors, falling within a very narrow range of only ∼1 kcal mol^{-1} for the individual catalysts (cf. Table S1 in the Supporting Information).

According to this analysis, the kinetics of the metallacycle growth is decisively determined by the strength of the M^{IV}−arene interaction in the metalla(IV)cycloalkane precursor **XC**. As the general trends elucidated, first, the extension of the C_1-bridge by an additional methylene group amplifies this interaction, thereby increasing the insertion barriers for the parent group 4 catalysts (Ar = C_6H_5, M = Zr, Hf) by approximately 4 and 5 kcal mol^{-1} ($\Delta\Delta G^{\ddagger}$, cf. Table 1), for the process with **7C** and **9C** as precursors, respectively. Notably, this gap becomes larger for donor-substituted catalysts, while electron-withdrawing groups reduce the gap. Second, a donor-functionalized hemilabile arene group acts to retard the insertion, while substituents that are electron-withdrawing cause the metallacycle growth kinetically more easily. Both trends are found to correlate well with the number as well as the donor−acceptor characteristic of the substituents (cf. Table 1). The manipulation of the electronic nature of the phenyl ring is seen to affect the kinetics of the insertion process for C_2-bridged catalysts to an exceptional extent ($\Delta\Delta G^{\ddagger}$ = ∼15 kcal mol^{-1}, for **7C** with η^5-Cp-(bridge)-$C_6H_3(CF_3)_2$ and η^5-Cp-(bridge)-$C_6H_2Me_3$ ligated catalysts, as an example), and to a lesser, but still remarkable ($\Delta\Delta G^{\ddagger}$ = ∼7.5 kcal mol^{-1}), extent for C_1-bridged systems (cf. Table 1). The stronger M^{IV}−arene interaction in **XC** for the first systems has been rationalized as being the origin.

The thermodynamics of the insertion process, however, is seen to be less influenced by modifications of the hemilabile arene functionality, as the thermodynamic driving force is predicted to fall into a rather narrow range (cf. Table 1). Overall, growth of the seven- and nine-membered zircona(IV)- and hafnia(IV)cycles is an exergonic process, such that thermodynamic grounds are not likely to prevent metallacycle growth.

B. Decomposition of Metallacycle Intermediates Affording α-Olefins. Decomposition of **7C** and **9C** into the 1-hexene−M^{II}, **7C-O**, and 1-octene−M^{II}, **9C-O**, products proceeds through the concerted β-H transfer occurring in close proximity to the metal. The key species involved along this process are shown in Figure 3, exemplified for CMe_2- and CMe_2CH_2-bridged Zr catalysts with the parent phenyl group (Ar = C_6H_5). Table 2 summarizes the energy profile for all investigated catalysts. The transition state encountered constitutes a quasi-planar arrangement of the $MC^{\beta}HC^{\alpha'}$ fragment, where the shifted hydrogen atom is at roughly equal distances from C^{β} and $C^{\alpha'}$ (cf. Figure 3). In contrast to the insertion step, here the pendant phenyl ligand assists the decomposition in two directions: first, to act to compensate for the reduction of the coordination sphere around the metal, thereby stabilizing the transition state coordinatively; second, to support the metal's low oxidation state in the α-olefin−M^{II} products **XC-O** (cf. Figure 3). Accordingly, the concerted β-H transfer should become accelerated for a hemilabile arene functionality that amplifies the M−arene interaction in the transition state effectively.

Again, we employed a simple isodesmic relation (cf. eq 1)[24] for the involved key species in order to obtain a more detailed insight into how electronic factors influence the kinetics of this elementary step. As already analyzed in the previous section, for the zircona(IV)- and the hafnia(IV)cycle precursors **7C** and **9C** the M^{IV}−arene interaction becomes amplified for systems with an enlarged C_2-bridge and also by a donor-functionalized phenyl group. Electron-withdrawing substituents, however, diminish the same interaction. Similar general trends are also found for the transition states for β-H transfer. As revealed from Table S2 (cf. Supporting Information package), donor substituents stabilize the transition state for both C_1- and C_2-bridged Zr- and Hf-based species to an extent that is similar to that found for the respective precursor **XC**. This results in energy profiles that are nearly congruous to the parent systems (Ar = C_6H_5), with relative barriers that vary by only ∼1−2 kcal mol^{-1} ($\Delta\Delta G^{\ddagger}$, cf. Table 2). For C_2-bridged catalysts with Ar = $C_6H_2Me_3$, unfavorable steric interactions between the *para*-methyl substituent and the metallacycle fragment cause a destabilization of the transition state that leads to slightly larger barriers for these cases. In contrast, the transition state is seen to be less stabilized relative to the precursor **XC** for

(25) For the catalysts investigated in this study (cf. Figure 1) the various substituents on the hemilabile phenyl group are likely to affect the individual elementary steps primarily by their electronic properties, while sterics are found to play a minor role. Steric pressure on the phenyl group, which, for instance, are due to unfavorable steric interactions of the terminal M−C bonds of the metallacycle fragment and/or of the incoming ethylene with *ortho*-phenyl substituents, have a pronounced influence on the energy profile. As exemplified for the insertion process, for catalysts with a pentamethyl-functionalized phenyl group (Ar = C_6Me_5), formation of the encounter complex and also ethylene insertion become disfavored relative to the counterparts bearing the η^5-Cp-(bridge)-$C_6H_2Me_3$ ligand. This causes the insertion barrier, in general, to increase by another ∼7−8 kcal mol^{-1}, which is essentially due to enhanced steric interactions. The influence of steric factors on the oligomerization reaction course, however, will be the subject of a forthcoming investigation.

(26) (a) Green, M. L. H. *J. Chem. Soc., Chem. Commun.* **1973**, 866. (b) Green, M. L. H. *J. Chem. Soc., Chem. Commun.* **1978**, 431. (c) Cloke, F. G. N.; Green, M. L. H. *J. Chem. Soc., Dalton Trans.* **1981**, 1938. (d) Cloke, G. *J. Chem. Soc., Chem. Commun.* **1987**, 1667. (e) Cotton, F. A.; Kibala, P. A.; Wojtczak, W. A. *J. Am. Chem. Soc.* **1991**, *113*, 1462. (f) Gillis, D. J.; Tudoret, M. J.; Baird, M. C. *J. Am. Chem. Soc.* **1993**, *115*, 2543. (g) Pellecchia, C.; Grassi, A.; Immirzi, A. *J. Am. Chem. Soc.* **1993**, *115*, 1160. (h) Bochmann, M.; Lancaster, S. J.; Hursthouse, M. B.; Malik, K. M. A. *Organometallics* **1994**, *13*, 2235. (i) Lancaster, S. J.; Robinson, O. B.; Bochmann, M.; Coles, S. J.; Hursthouse, M. B. *Organometallics* **1995**, *14*, 2456.

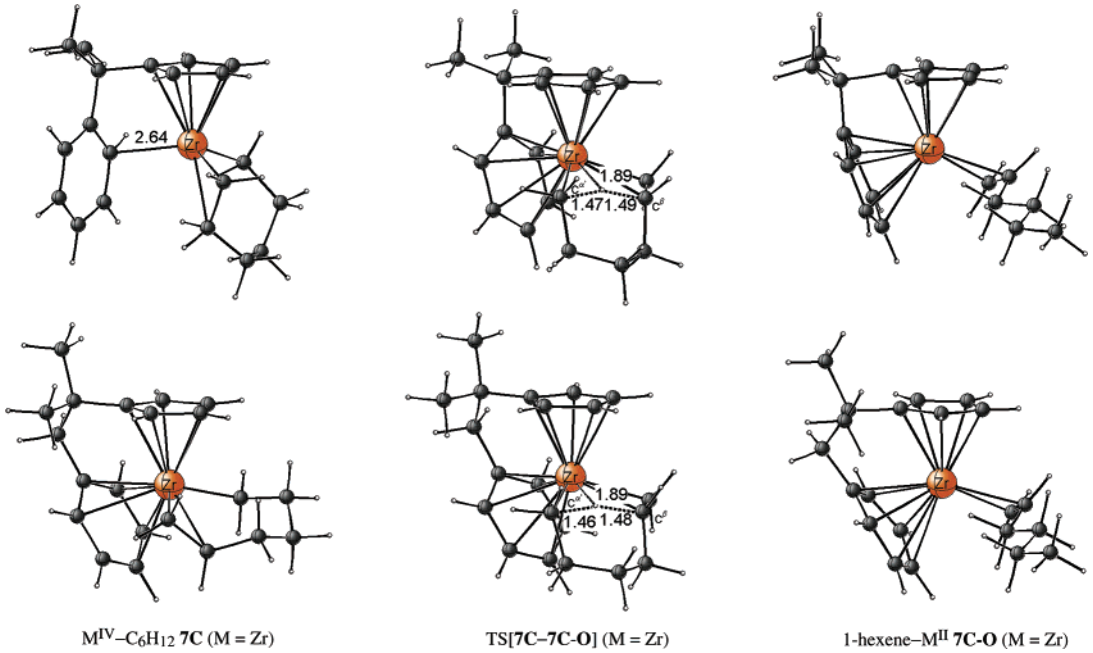

Figure 3. Selected geometric parameters (Å) of the optimized structures of key species for decomposition of the metalla-(IV)cycloheptane **7C** into the 1-hexene−M^{II} complex **7C-O** through concerted transition-metal-assisted β-H transfer, for CMe_2-bridged (top) and CMe_2CH_2-bridged (bottom) systems.[23] See Figure 2.

Table 2. Calculated Gibbs Free-Energy Profile (ΔG, $\Delta G^{\ddagger}$ in kcal mol^{-1}) for Decomposition of Group 4 Metallacycle Intermediates Affording α-Olefins during the Linear Oligomerization of Ethylene Mediated by the Cationic $[(\eta^5\text{-}C_5H_4\text{-}(CMe_2R'\text{-bridge})\text{-}C_6H_xR_y)M^{II}(C_2H_4)_2]^+$ (M = Zr, Hf) Active Catalyst Complex[a,23]

cycle decomposition	arene functionality	$\Delta G^{\ddagger}$ M = Zr/Hf	ΔG M = Zr/Hf
$M^{IV}-C_6H_{12} \rightarrow$ 1-hexene−M^{II}	C_6H_5	13.1/17.4	−9.0/−3.7
7C → 7C-O	$C_6H_2F_3$	16.1/20.5	−5.1/0.0
CMe_2-bridge	$C_6H_3(CF_3)_2$	16.9/21.5	−8.3/−3.2
	$C_6H_3Me_2$	12.2/16.4	−9.9/−5.0
	$C_6H_2Me_3$	13.0/17.3	−7.8/−2.9
CMe_2CH_2-bridge	C_6H_5	9.8/14.8	−11.2/−6.2
	$C_6H_2F_3$	10.6/15.1	−10.1/−5.5
	$C_6H_3(CF_3)_2$	10.5/15.3	−17.8/−13.8
	$C_6H_3Me_2$	11.3/16.9	−10.4/−4.8
	$C_6H_2Me_3$	13.0/18.6	−8.3/−2.7
$M^{IV}-C_8H_{16} \rightarrow$ 1-octene−M^{II}	C_6H_5	16.1/20.1	−15.3/−10.1
9C → 9C-O	$C_6H_2F_3$	19.7/23.0	−11.3/−6.6
	$C_6H_3(CF_3)_2$	19.6/23.3	−15.7/−11.1
	$C_6H_3Me_2$	16.9/19.4	−15.6/−12.2
	$C_6H_2Me_3$	17.9/20.4	−13.4/−10.0
CMe_2CH_2-bridge	C_6H_5	16.3/18.9	−14.9/−12.3
	$C_6H_2F_3$	17.6/20.0	−14.0/−11.4
	$C_6H_3(CF_3)_2$	16.7/19.1	−22.0/−20.5
	$C_6H_3Me_2$	17.1/19.9	−14.8/−11.8
	$C_6H_2Me_3$	17.8/21.2	−13.2/−9.5

[a] The activation and reaction free energies for individual processes are given for Zr-/Hf-based catalysts, respectively, relative to the corresponding metallacycle precursor **XC**.

catalysts with an acceptor-substituted arene group. This is most pronounced for Zr and Hf catalysts with a C_1-bridge, giving rise to a kinetically more difficult β-H transfer having barriers that are ∼3−4 kcal mol^{-1} ($\Delta\Delta G^{\ddagger}$, cf. Table 2) higher than for the parent catalysts (Ar = C_6H_5), but less effective for the corresponding C_2-bridged systems having predicted barriers that are very similar to the parent catalyst.

Different from the insertion process, where the strength of the M−arene interaction in the precursor **XC** is the crucial factor that determines the kinetics, the barrier for β-H transfer is essentially controlled by the ability of the hemilabile arene functionality to stabilize the transition state coordinatively. The decomposition of **7C** becomes facilitated kinetically for Zr and Hf catalysts with an enlarged C_2-bridge, as indicated by the reduction of the barrier for the parent catalysts (Ar = C_6H_5) by ∼3 kcal mol^{-1} ($\Delta\Delta G^{\ddagger}$, relative to the C_1-bridged congeners, cf. Table 2). The similar energy profiles predicted for C_1- and C_2-bridged parent catalysts (Ar = C_6H_5, M = Zr, Hf) in the process commencing from **9C** reveal the minor influence of the bridge length in this case. Here, unfavorable steric interactions between the C_2-bridged phenyl group and the metalla(IV)cyclononane fragment come into play, which counterbalance the coordinative stabilization of TS[**9C-9C-O**]. Overall, the modification of the electronic nature of the hemilabile arene functionality is indicated as having only a modest influence on the energetics of the decomposition step. The donor ability of the substituent is the crucial electronic factor for the stabilization of the transition state, thereby acting to accelerate the β-H transfer. For the catalysts with methyl-substituted arene functionalities probed in the present investigation, however, both the precursor **XC** and the transition state are supported to an almost identical extent, in the absence of unfavorable steric interactions, thus affecting the kinetics and the thermodynamics in a less pronounced fashion. With regard to electronic factors, the decomposition is predicted to become kinetically more complicated with electron-withdrawing substituents, due to a less efficient M−arene interaction in the transition state.

Scheme 2. Condensed Gibbs Free-Energy Profile (kcal mol^{-1}) of Competing Metallacycle Growth and Decomposition Steps of the Linear Oligomerization of Ethylene by the Cationic [(η^5-Cp-(CMe$_2$-bridge)-C$_6$H$_x$R$_y$)M^{II}(C$_2$H$_4$)$_2$]$^+$ (M = Zr) Active Catalyst[a]

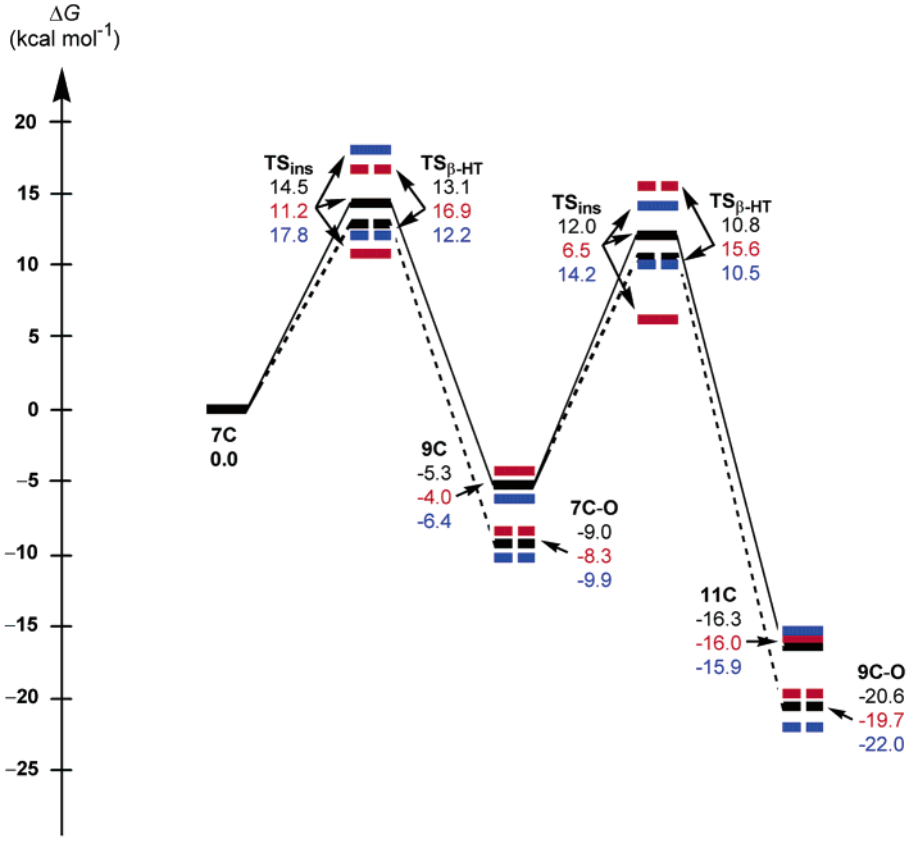

[a] Exemplified for **7C** and **9C** as the precursors, respectively, with **7C** chosen as reference. The profiles for catalysts with the parent (Ar = C$_6$H$_5$), the acceptor-substituted (Ar = C$_6$H$_3$(CF$_3$)$_2$), and the donor-substituted (Ar = C$_6$H$_3$Me$_2$) hemilabile arene functionalities are marked in black, red, and blue, respectively. Bold and broken lines indicate key species along growth and decomposition paths, respectively.

II. Influence of Modifications of the Hemilabile Arene Functionality on the Catalyst's Potential for Linear Oligomerization of Ethylene. Having elucidated the influence of modifications of the hemilabile arene functionality on the energetics for the metallacycle growth and decomposition processes, the first of which has been shown to be affected to a larger extent, the potential of the investigated systems as efficient catalysts for oligomerization of ethylene to higher linear α-olefins is analyzed next. The oligomer product distribution has been shown in our previous study[13b] to be almost entirely regulated by the relative kinetics for the competing growth and decomposition steps ($\Delta\Delta G^{\ddagger}_{d-g}$),[27] where **7C** and **9C** are the crucial precursors for production of α-olefins in the valuable range of C$_6$−C$_{18}$. The condensed free-energy profiles for the investigated Zr and Hf catalysts bearing CMe$_2$- and CMe$_2$CH$_2$-bridges are presented in Schemes 2−5, respectively. These schemes comprise the growth and the decomposition of **7C** and **9C**, exemplified for the parent (Ar = C$_6$H$_5$) catalysts and for catalysts with prototypical donor- (Ar = C$_6$H$_3$Me$_2$) and acceptor-substituted (Ar = C$_6$H$_3$(CF$_3$)$_2$) arene functionalities. The composition of the α-olefin products is estimated from a simple kinetic model that employs the computed barriers. Tables 3 and 4 collect the estimated oligomer distribution and the relative thermodynamic abundance of various metallacycle intermediates, respectively, for all investigated catalysts; further details are given elsewhere.[13b]

The parent (Ar = C$_6$H$_5$) C$_1$-bridged Zr system has been suggested in a recent computational study[13b] as a promising catalyst possessing abilities for production of 1-octene besides the prevalent 1-hexene oligomer product. As revealed from Scheme 2, here, both **7C** and **9C** exhibit a slightly higher propensity for decomposition than for growth. The computed $\Delta\Delta G^{\ddagger}_{d-g}$ gap[27] of only −1.4 kcal mol^{-1} for **7C**, however, indicates a certain probability for formation of **9C**, thereby giving rise to a 1-hexene/1-octene oligomer mixture, with 1-hexene as the major product (cf. Table 3). For the related catalysts bearing arene functionalities with electron-releasing substituents, which act to accelerate slightly the concerted β-H transfer and retarding insertion (cf. sections I.A, I.B), the $\Delta\Delta G^{\ddagger}_{d-g}$ gap becomes significantly increased for both **7C** and **9C**, making the β-H transfer the more favorable process. The predicted $\Delta\Delta G^{\ddagger}_{d-g}$ gap of >−5 kcal mol^{-1} (cf. Scheme 2) is likely to be large enough to prevent further growth of **7C**, thereby switching the parent Zr system into a highly selective catalyst for ethylene trimerization, as evident from the estimated product composition (cf. Table 3). As a further relevant aspect, the available catalytic species are consumed almost quantitatively for production of 1-hex-

(27) The $\Delta\Delta G^{\ddagger}_{d-g}$ value represents the difference of the free-energy barriers for competing decomposition and growth steps for a particular metallacycle intermediate.

Scheme 3. Condensed Gibbs Free-Energy Profile (kcal mol^{-1}) of Competing Metallacycle Growth and Decomposition Steps of the Linear Oligomerization of Ethylene by the Cationic [(η^5-Cp-(CMe_2CH_2-bridge)-$C_6H_xR_y$)$M^{II}(C_2H_4)_2$]$^+$ (M = Zr) Active Catalyst[a]

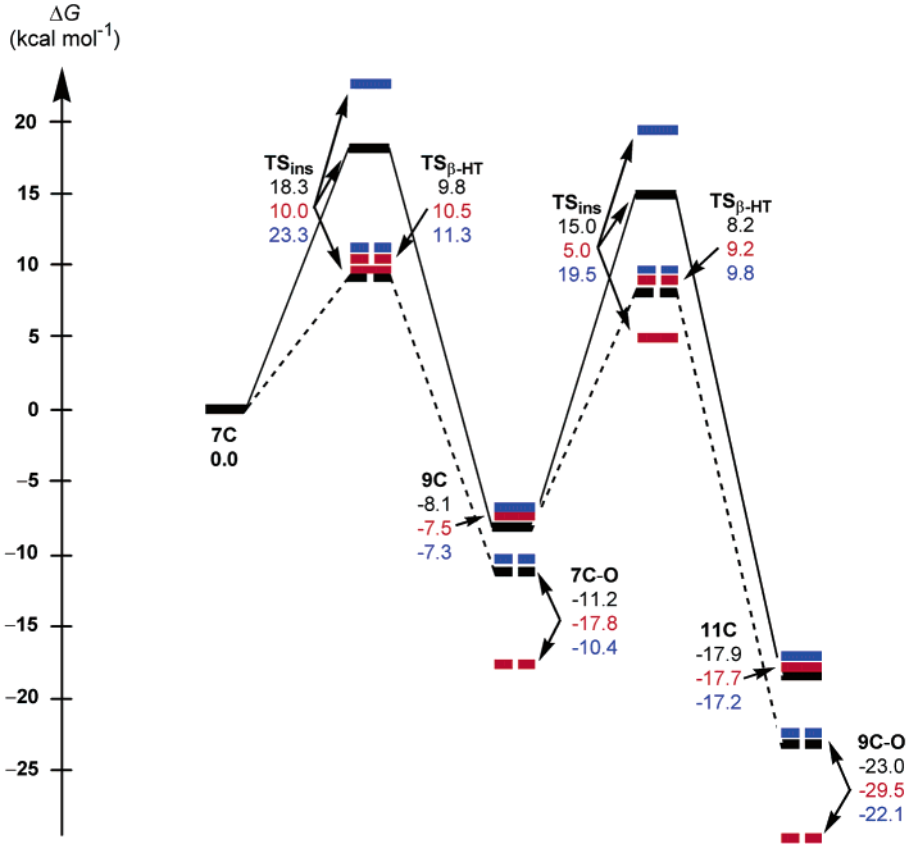

[a] See Scheme 2.

ene, since the thermodynamic population of **9C** and larger zircona(IV)cycles is likely to be very small (cf. Table 4). Modification of the arene functionality with electron-withdrawing substituents also gives rise to a larger $\Delta\Delta G^{\ddagger}_{d-g}$ gap of 5.7 and 9.1 kcal mol^{-1} for **7C** and **9C** (Ar = $C_6H_3(CF_3)_2$, cf. Scheme 2), respectively, with the zircona(IV)cycles exhibiting a distinctly greater propensity for further growth, due to the accelerated ethylene insertion (cf. section I.A). As a result, almost all available catalytic species are transformed into larger zircona(IV)cycle intermediates and only a negligible amount (<1%, cf. Table 4) undergoes decomposition into 1-hexene and/or 1-octene. The ability for decomposition has been shown to decrease for larger metallacycles.[13b] Accordingly, α-olefins in the valuable range of C_6-C_{18} are less likely to occur in the oligomer distribution, which should predominantly consist of long chain oligomer/polymer products. To summarize, donor-functionalized Zr catalysts with a C_1-bridge are suggested to display catalytic abilities for the selective ethylene trimerization to 1-hexene. These systems likely have an activity that is comparable to that of the reported parent (Ar = C_6H_5) Ti catalyst,[12b] due to predicted similar barriers for the rate-determining ethylene insertion into the metalla(IV)cyclopentane.[28] On the other hand, long chain oligomers/polymers (having chain lengths $\gg C_{20}$) can be expected as the major products for C_1-bridged Zr catalysts with electron-withdrawing substituents on the arene group.

The influence of the extended bridge on the kinetics of the two competing steps, analyzed in previous sections, leads to the following variation in the catalytic abilities of Zr catalysts (cf. Schemes 2 and 3). As apparent from Table 3, the ability of the parent (Ar = C_6H_5) system with an C_1-bridge will switch from oligomerization affording a 1-hexene/1-octene mixture to ethylene trimerization for the C_2-bridged system, due to an increased $\Delta\Delta G^{\ddagger}_{d-g}$ gap of −8.5 kcal mol^{-1} for **7C** (cf. Scheme 3). Moreover, the preference of the donor-functionalized C_1-bridged catalysts for the selective generation of 1-hexene is enhanced further ($\Delta\Delta G^{\ddagger}_{d-g}$ = −5.6 and −12.0 kcal mol^{-1} for **7C** with C_1- and C_2-bridged catalysts, respectively, with Ar = $C_6H_3Me_2$). As mentioned in section I.A, a C_2-bridged donor-functionalized arene group gives rise to a kinetically more difficult ethylene insertion. The corresponding catalysts will exhibit a lower activity for trimerization than the congeners with a C_1-bridge (vide supra), as indicated by the predicted discriminating barrier.[28] A product mixture containing 1-hexene and long chain oligomers/polymers is suggested for acceptor-substituted catalysts

(28) The ethylene insertion into the metalla(IV)cyclopentane is the rate-controlling step for ethylene trimerization to 1-hexene (refs 13a,b). This step is connected with an activation energy of 15.6 kcal mol^{-1} ($\Delta G^{\ddagger}$) for the experimentally reported Ti catalyst (Ar = C_6H_5, ref 13b), while it has free-energy barriers of 14.0/15.4 kcal mol^{-1} (M = Zr/Hf, C_1-bridge, Ar = $C_6H_3Me_2$), 15.4/17.0 kcal mol^{-1} (M = Zr/Hf, C_1-bridge, Ar = $C_6H_2Me_3$), 16.1/17.4 kcal mol^{-1} (M = Zr/Hf, C_2-bridge, Ar = C_6H_5), 21.4/23.2 kcal mol^{-1} (M = Zr/Hf, C_2-bridge, Ar = $C_6H_3Me_2$), and 22.3/24.0 kcal mol^{-1} (M = Zr/Hf, C_2-bridge, Ar = $C_6H_2Me_3$) for the various selective 1-hexene-generating Zr and Hf catalysts, respectively.

Scheme 4. Condensed Gibbs Free-Energy Profile (kcal mol^{-1}) of Competing Metallacycle Growth and Decomposition Steps of the Linear Oligomerization of Ethylene by the Cationic [(η^5-Cp-(CMe$_2$-bridge)-C$_6$H$_x$R$_y$)M^{II}(C$_2$H$_4$)$_2$]$^+$ (M = Hf) Active Catalyst[a]

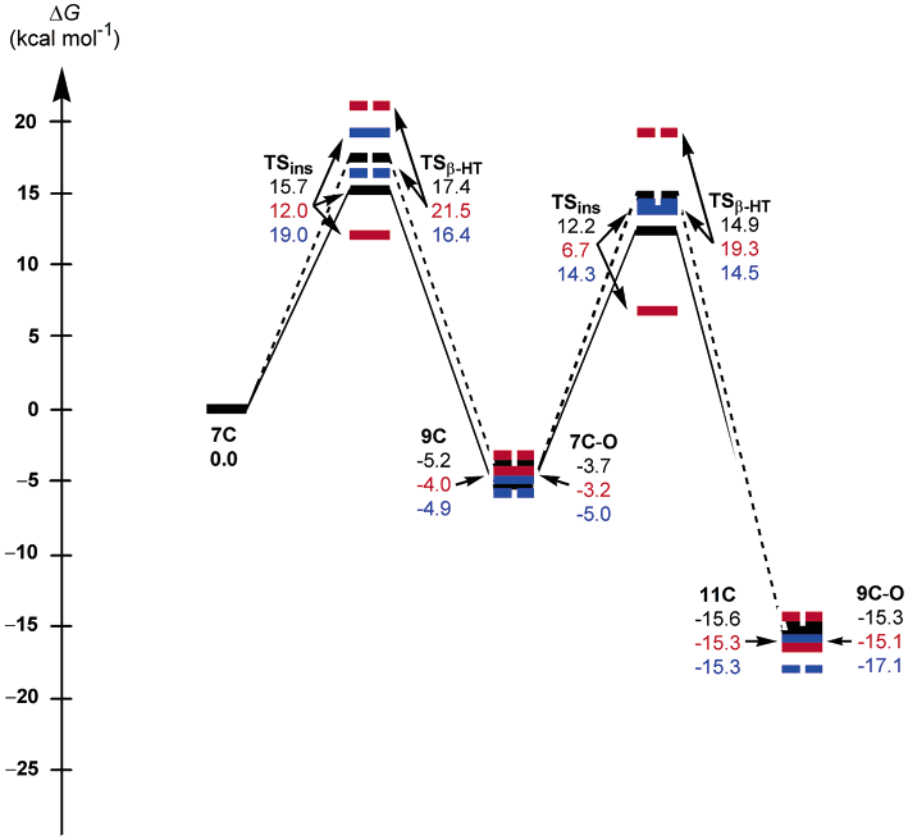

[a] See Scheme 2.

(cf. Tables 3, 4). Overall, neither the electronic modification of the hemilabile arene functionality nor an extended bridge, probed computationally for Zr-based oligomerization catalysts, is indicated to increase the 1-octene portion or to enhance significantly the catalytic activity for ethylene trimerization beyond what is already reached for the reported Ti catalyst.[12b,28]

As demonstrated in our previous study,[13b] the concerted β-H transfer becomes kinetically more difficult for Hf-based catalysts, due to the increase in the M−C bond strength upon descending group 4. On the other hand, comparable energetics are predicted for the ethylene insertion into the Zr−C and Hf−C bonds of the metallacycle intermediates. For the parent (Ar = C$_6$H$_5$) Hf catalyst with a C$_1$-bridge, this results in a higher aptitude of **7C** ($\Delta\Delta G^{\ddagger}_{d-g}$ = 1.7 kcal mol^{-1}, cf. Scheme 4) and **9C** ($\Delta\Delta G^{\ddagger}_{d-g}$ = 2.7 kcal mol^{-1}) for subsequent growth than for decomposition, with the $\Delta\Delta G^{\ddagger}_{d-g}$ gap increasing further for larger hafnia(IV)cycles.[13b] As revealed from Table 3, this system exhibits a low productivity for generation of C$_6$−C$_{18}$ α-olefins, since the majority of the catalytically active species are converted into large hafnia(IV)cycles (of sizes ≫C$_{20}$, cf. Table 4), affording long chain oligomers/polymers as the predominant products. The individual steps are affected by electronic factors in a fashion similar to that already discussed for the Zr counterparts. This leads to a significantly increased $\Delta\Delta G^{\ddagger}_{d-g}$ gap for acceptor-functionalized catalysts (cf. Scheme 4), with the ethylene insertion strongly preferred kinetically, thereby indicating long chain oligomers/polymers as the prevalent products (cf. Table 4).

On the other hand, donor substituents are seen to change the abilities of the hafnia(IV)cycle precursors. Decomposition of **7C** becomes more facile than ethylene insertion ($\Delta\Delta G^{\ddagger}_{d-g}$ = −2.6 kcal mol^{-1}, Ar = C$_6$H$_3$Me$_2$), while a very similar propensity for the two steps is predicted for **9C**. Similar to the findings for the Zr catalysts, this pushes the Hf systems with a donor-substituted arene group into the class of catalysts for ethylene trimerization (cf. Table 3). The comparison of the discriminating barrier for the trimerization course for donor-functionalized Zr and Hf catalysts reveals the C$_1$-bridged Hf systems, however, as the less efficient trimerization catalysts.[28]

The larger C$_2$-bridge affects the catalytic abilities of the Hf-based systems in a fashion very similar to that already described for the Zr counterparts (cf. Scheme 5). It turns the parent (Ar = C$_6$H$_5$) catalyst as well the systems bearing donor groups on the arene functionality into selective, but less active, trimerization catalysts (cf. Table 3).[28] On the other hand, the modification with electron-withdrawing substituents, will, similar to the C$_1$-bridged counterparts, almost entirely give rise to long chain oligomers/polymers as the products (cf. Table 4).

Concluding Remarks

We have presented a detailed theoretical analysis of the influence of modifications of the hemilabile arene

Scheme 5. Condensed Gibbs Free-Energy Profile (kcal mol^{-1}) of Competing Metallacycle Growth and Decomposition Steps of the Linear Oligomerization of Ethylene by the Cationic [(η^5-Cp-(CMe_2CH_2-bridge)-$C_6H_xR_y$)$M^{II}(C_2H_4)_2$]$^+$ (M = Hf) Active Catalyst[a]

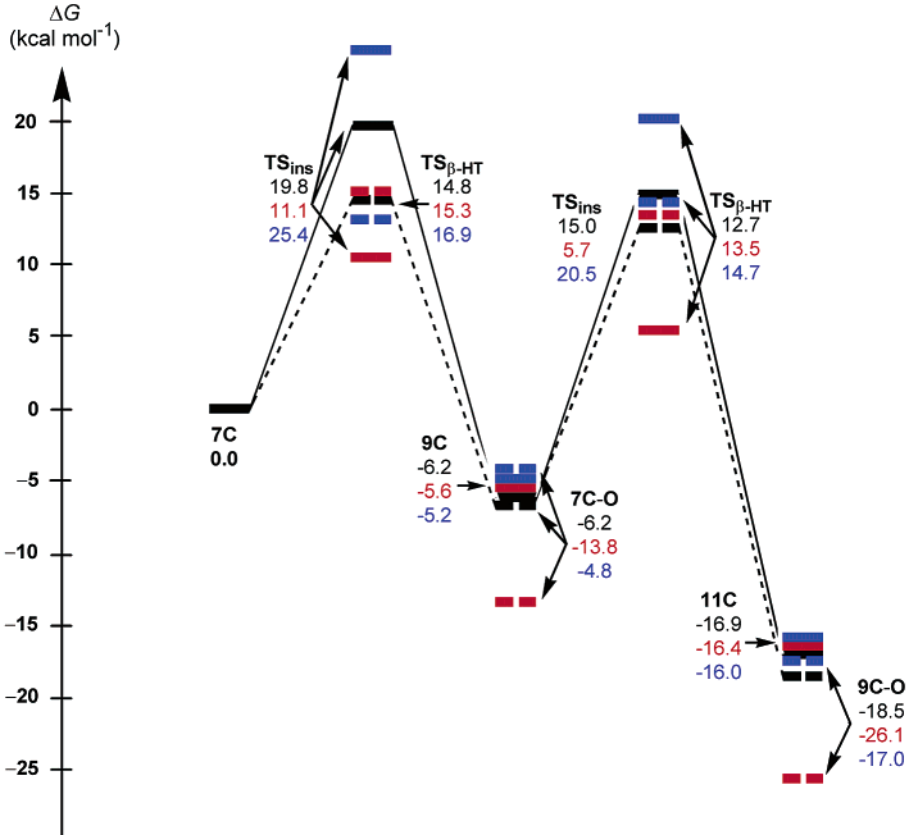

[a] See Scheme 2.

Table 3. Estimated Composition of the α-Olefin Products for the Linear Oligomerization of Ethylene Mediated by the Cationic [(η^5-C_5H_4-(CMe_2R'-bridge)-$C_6H_xR_y$)$M^{II}(C_2H_4)_2$]$^+$ (M = Zr, Hf) Active Catalyst Complex[23]

%(α-olefin)[a]	arene functionality	1-hexene M = Zr/Hf	1-octene M = Zr/Hf
CMe_2-bridge	C_6H_5	91.4/5.4	7.6/1.0
	$C_6H_2F_3$	0.3/1.4 × 10^{-3}	2.1 × 10^{-2}/1.1 × 10^{-4}
	$C_6H_3(CF_3)_2$	6.5 × 10^{-3}/ 1.1 × 10^{-5}	2.1 × 10^{-5}/5.7 × 10^{-8}
	$C_6H_3Me_2$	100.0/98.8	7.8 × 10^{-3}/0.5
	$C_6H_2Me_3$	100.0/98.3	1.1 × 10^{-2}/0.5
CMe_2CH_2-bridge	C_6H_5	100.0/100.0	5.8 × 10^{-5}/2.1 × 10^{-2}
	$C_6H_2F_3$	98.3/10.0	0.8/0.1
	$C_6H_3(CF_3)_2$	30.1/8.3 × 10^{-2}	5.8 × 10^{-2}/1.9 × 10^{-4}
	$C_6H_3Me_2$	100.0/100.0	1.6 × 10^{-7}/5.8 × 10^{-5}
	$C_6H_2Me_3$	100.0/100.0	2.2 × 10^{-7}/6.9 × 10^{-5}

[a] Portions of individual α-olefins in the product mixture; for details see ref 13b.

functionality on the catalytic abilities of Zr- and Hf-based cationic [(η^5-Cp-(CMe_2R'-bridge)-$C_6H_yR_x$)$M^{II}(C_2H_4)_2$]$^+$ active species as efficient catalysts for linear ethylene oligomerization, employing a gradient-corrected DFT method. The modifications that were probed computationally comprised the arene substitution by prototypic electron-releasing (R = Me) and electron-withdrawing (R = F, CF_3) groups in various patterns (cf. Figure 1) and also the extension of the Cp-arene connecting bridge by an additional methylene group (R′ = CH_2). The Ti system with an unsubstituted (Ar = C_6H_5) CMe_2-bridged phenyl group has been shown experimentally to be a highly selective catalyst for ethylene trimerization,[12a,b] the origin of which has been elucidated in a previous theoretical mechanistic study.[13a] The corresponding catalysts with the heavier group 4 metals Zr and Hf as the active center, which have not been reported so far by experimental groups, have recently been explored computationally. These studies suggested that the Zr system (Ar = C_6H_5) might be a promising catalyst capable of producing 1-octene besides the prevalent 1-hexene.[13b] The present computational study was aimed at enhancing the understanding of the catalytic structure−reactivity relationships further by elucidating how electronic factors (first) affect the crucial metallacycle growth and decomposition steps and (second) act to regulate the catalytic activity and selectivity, thereby contributing to the computer-based rational design of improved group 4 catalysts of the title class for either the selective generation of 1-hexene or the production of increased portions of 1-octene in the oligomer product mixture. To the best of our knowledge, this is the first comprehensive theoretical exploration of variations in the ligand backbone for group 4 oligomerization catalysts, where all crucial elementary steps of the catalytic cycle have been critically scrutinized.

The kinetics of the metallacycle growth has been shown to be decisively determined by the strength of the M^{IV}−arene interaction in the metallacycle precursors **XC**. The first phenyl group displacement by incoming ethylene is seen to contribute mostly to the relative overall barriers for this step, while the intrinsic insertion barrier is less affected by electronic factors. As the

Table 4. Estimated Abundance of Various Metallacycle Intermediates in the Reaction Course of the Linear Oligomerization of Ethylene Mediated by the Cationic $[(\eta^5\text{-}C_5H_4\text{-}(CMe_2R'\text{-bridge})\text{-}C_6H_xR_y)M^{II}(C_2H_4)_2]^+$ (M = Zr, Hf) Active Catalyst Complex[23]

$[M^{IV}-C_nH_{2n}]^a$	arene functionality	$M^{IV}-C_4H_8$ M = Zr/Hf	$M^{IV}-C_6H_{12}$ M = Zr/Hf	$M^{IV}-C_8H_{16}$ M = Zr/Hf	$M^{IV}-C_{10}H_{20}$ M = Zr/Hf
CMe_2-bridge	C_6H_5	100/100	100/100	8.6/94.6	1.0/93.7
	$C_6H_2F_3$	100/100	100/100	99.7/100	99.7/100
	$C_6H_3(CF_3)_2$	100/100	100/100	99.9/100	99.9/100
	$C_6H_3Me_2$	100/100	100/100	7.8×10^{-3}/1.2	1.5×10^{-5}/0.7
	$C_6H_2Me_3$	100/100	100/100	1.1×10^{-2}/1.7	4.9×10^{-5}/1.3
CMe_2CH_2-bridge	C_6H_5	100/100	100/100	$5.8 \times 10^{-5}/2.1 \times 10^{-2}$	$6.0 \times 10^{-10}/2.2 \times 10^{-4}$
	$C_6H_2F_3$	100/100	100/100	1.7/90.0	0.9/89.9
	$C_6H_3(CF_3)_2$	100/100	100/100	69.9/99.9	69.9/99.2
	$C_6H_3Me_2$	100/100	100/100	$1.6 \times 10^{-7}/5.8 \times 10^{-5}$	$1.2 \times 10^{-14}/3.2 \times 10^{-9}$
	$C_6H_2Me_3$	100/100	100/100	$2.2 \times 10^{-7}/6.9 \times 10^{-5}$	$2.4 \times 10^{-14}/6.4 \times 10^{-9}$

[a] Thermodynamic abundance of different sized metallacycles, with an assumed thermodynamic population of 100 for the metalla(IV)-cyclopentane $M^{IV}-C_4H_8$; for details see ref 13b.

general trends elucidated for Zr and Hf systems, the extension of the C_1-bridge by an additional methylene group amplifies this interaction, thereby acting to reduce the tendency for formation of the ethylene encounter complex and to increase the barrier for ethylene insertion. The electronic modification of the arene functionality by electron-releasing/-withdrawing substituents strengthen/weaken this interaction in **XC**, giving rise to a lower/higher abundance of the ethylene π-adducts and also to kinetically less/more facile insertion steps, respectively. All these trends were found to correlate well with the number as well as the donor−acceptor characteristic of the substituents.

Different from the insertion step, the barrier for β-H transfer is essentially controlled by the ability of the arene functionality to stabilize the transition state coordinatively. Decomposition of **7C** (M = Zr, Hf) was found to be facilitated by the larger C_2-bridge, which, however, affects the process commencing from **9C** in a less pronounced fashion, as here sterics are coming into play. The donor ability of the substituent is the crucial electronic factor for the coordinative stabilization of the transition state by the phenyl group, thereby acting to accelerate the decomposition step. The opposite influence has been elucidated for substituents that are electron-withdrawing.

Among the two crucial elementary processes, the ethylene insertion has been analyzed to be affected to a distinctly larger extent by the probed modifications of the hemilabile arene functionality.

With regard to the catalytic potential of the Zr- and Hf-based systems, the introduction of electron-releasing substituents into the arene functionality and also the enlarged C_2-bridge force the parent (Ar = C_6H_5) C_1-bridged systems into selective catalysts for ethylene trimerization. These Zr catalysts might have an activity that is comparable to the reported Ti catalyst (C_1-bridge, Ar = C_6H_5),[12b] while the related Hf systems are less active. On the other hand, Zr catalysts with an acceptor-functionalized phenyl group are likely to lose the ability for generation of α-olefins in the valuable range of C_6-C_{18} chain lengths, and instead long chain oligomers/polymers are produced. The already small productivity of the parent (Ar = C_6H_5) Hf system for formation of C_6-C_{18} α-olefins becomes reduced further by a acceptor-modified arene functionality.

Unfortunately, neither of the probed modifications of the hemilabile arene functionality can be suggested as improvements for enhancing the catalytic abilities of the title group 4 catalysts toward increasing the portion of 1-octene or leading to a significantly higher catalytic activity for ethylene trimerization to exceed that reported for the Ti catalyst.

Acknowledgment. Support from the National Science and Engineering Research Council of Canada (NSERC) is gratefully acknowledged. T.Z. wishes to thank the Canadian government for a Canada research chair in theoretical inorganic chemistry.

Supporting Information Available: Full descriptions of the geometry of all reported species (Cartesian coordinates in Å) and the collection of relative stabilities of the key species for all investigated catalysts (Tables S1 and S2). This material is available free of charge via the Internet at http://pubs.acs.org.

OM0498100